Characterization of the clade 4 non-toxigenic *C. difficile* isolate L-NTCD03 carrying the *cfr*(B) gene

Britt Nibbering[1], Sam Nooij[1,2], Céline Harmanus[2], Ingrid M.J.G. Sanders[2], Inez M. Miedema[2], Quinten R. Ducarmon[1,2], Rolf H.A.M. Vossen[3], Susan L. Kloet[3], Colleen K. Ardis[4], Robert A. Britton[4], Farnaz Yousefi[5], Jenna Bayne[6,7], C. Charavaryamath[8,9], Andy Law[10], Morgan L. Murphy[10,11], Brett Sponseller[12,13], Eric R. Burrough[7], Shankumar Mooyottu[5,14], Tanja Opriessnig[7,15], Ed J. Kuijper[1,2], Meta Roestenberg[16], Wiep Klaas Smits [1,2,*]

[1] Centre for Microbiome Analyses and Therapeutics, Leiden University Center for Infectious Diseases (LUCID), Leiden University Medical Center, Leiden, The Netherlands

[2] Experimental Bacteriology, Leiden University Center for Infectious Diseases (LUCID), Leiden University Medical Center, Leiden, The Netherlands

[3] Leiden Genome Technology Center, Department of Human Genetics, Leiden University Medical Center, Leiden, The Netherlands

[4] Therapeutic Microbiology Laboratory, Department of Molecular Virology and Microbiology, Alkek Center for Metagenomics and Microbiome Research, Baylor College of Medicine, Houston TX, USA

[5] Department of Pathobiology, College of Veterinary Medicine, Auburn University, Auburn, AL, USA

[6] Department of Clinical Sciences, College of Veterinary Medicine, Auburn University, Auburn, AL, USA

[7] Department of Veterinary Diagnostic and Production Animal Medicine, College of Veterinary Medicine, Iowa State University, Ames, IA, USA

[8] Department of Biomedical Sciences, College of Veterinary Medicine, Iowa State University, Ames, IA, USA

[9] Department of Veterinary Biomedical Sciences, Shreiber School of Veterinary Medicine, Rowan University, Glassboro, NJ, USA

[10] Department of Veterinary Clinical Sciences, College of Veterinary Medicine, Iowa State University, Ames, IA, USA

[11] Department of Veterinary Medicine and Surgery, College of Veterinary Medicine, University of Missouri, Columbia, MO, USA

[12] Department of Veterinary Microbiology and Preventive Medicine, College of Veterinary Medicine, Iowa

29 State University, Ames, IA, USA.

30 [13] Department of Veterinary Science, Martin-Gatton College of Agriculture, Food and Environment, University

31 of Kentucky, Lexington, KY, USA

32 [14] Department of Veterinary Pathology, College of Veterinary Medicine, Iowa State University, Ames, IA, USA

33 [15] Department of Vaccines and Diagnostics, the Moredun Research Institute, Edinburgh, UK.

34 [16] Controlled Human Infections Center, Leiden University Center for Infectious Diseases, Leiden University

35 Medical Center, Leiden, The Netherlands

36

37 **Running title**: Characterization of L-NTCD03

38 **Key words**: non-toxigenic *C. difficile*, complete genome, antimicrobial resistance, nutrient utilization

39

40 * Corresponding author: Experimental Bacteriology group, Leiden University Center for Infectious Diseases,

41 Leiden University Medical Center, PO Box 9600, 2300RC, Leiden, The Netherlands, phone: +31-71-526 1229,

42 fax: +31-71-526 6761, E-mail: w.k.smits@lumc.nl

43

44

Abstract

Clostridioides difficile infection (CDI) is a toxin-mediated gastro-intestinal disease. Yet, *C. difficile* is a phylogenetically diverse species that includes many non-toxigenic strains. In general, these are understudied, despite having significant potential impact for our understanding of the colonization process and as therapeutic modalities. Here, we present an in-depth characterization – including the complete genome sequence - of the non-toxigenic *C. difficile* strain L-NTCD03. This strain belongs to PCR ribotype 416, clade 4 and multilocus sequence type 39. It is resistant to multiple antimicrobials, but not those used for treatment of CDI. We validated the relevance of the *cfr*(B) gene from this strain in antimicrobial resistance to clindamycin, linezolid, retapamulin and streptogramin A. We found the L-NTCD03 strain to be non-toxic in various assays. Altogether, L-NTCD03 is a promising candidate for developing into a live biotherapeutic product.

Introduction

The Gram-positive anaerobic spore-forming bacterium *Clostridioides difficile* is best known as a nosocomial pathogen and *C. difficile* infection (CDI) is regarded as an important cause of healthcare-associated infectious diarrhea (Leffler & Lamont, 2015, Smits *et al.*, 2016). In this context, in particular strains belonging to the fluoroquinolone resistant PCR ribotype 027 (RT027) are associated with increased morbidity and mortality (Warny *et al.*, 2005, He *et al.*, 2013). Nevertheless, recent years have seen an increase in CDI cases that are not linked to classical risk factors such as antibiotic use or healthcare exposure, and are community-acquired (Smits *et al.*, 2016, Viprey *et al.*, 2022). Strains belonging to different types than RT027, such as those belonging PCR ribotype 078 (RT078), which also occur in many animal species, may be associated with community-acquired disease (Goorhuis *et al.*, 2008, Viprey *et al.*, 2022). Thus, *C. difficile* can be considered a quintessential One Health pathogen (Lim *et al.*, 2020).

Considering its causative role in debilitating disease, much research has focused on the main virulence factors of *C. difficile:* toxin A (TcdA), toxin B (TcdB) and binary toxin (CDT) (Aktories *et al.*, 2017, Kordus *et al.*, 2022). Of note, whereas TcdA and/or TcdB is required for disease, CDT is mainly produced by a subset of

73 toxigenic *C. difficile* strains, including those belonging to the epidemic types RT027 and RT078 (Smits *et al.*,
74 2016).

75 *C. difficile* colonization does not always lead to disease. Importantly, a fraction of the population is
76 asymptomatically colonized by toxigenic *C. difficile* (Crobach *et al.*, 2018) and in particular in infants a high
77 prevalence of *C. difficile* is noted without apparent disease (Ferretti *et al.*, 2023, Mani *et al.*, 2023).
78 Additionally, *C. difficile* is not a universally pathogenic species; that is, non-toxigenic *C. difficile* (NTCD) strains
79 exist that lack the genes encoding TcdA, TcdB and CDT, such as those belonging to PCR ribotype 010 (RT010)
80 (Braun *et al.*, 1996, Monot *et al.*, 2015, Smits *et al.*, 2016). Though these isolates have not been found to
81 induce disease in humans and animals, it has been noted that they might act as reservoirs for antimicrobial
82 resistance genes. For instance, resistance to metronidazole is common in RT010 strains (Boekhoud *et al.*, 2020,
83 Boekhoud *et al.*, 2021) and over half the non-toxigenic isolates from Southeast Asia appeared to carry
84 antimicrobial resistance determinants on mobile genetic elements (Imwattana *et al.*, 2020).

85 *C. difficile* is a phylogenetically diverse species with isolates falling into at least 5 classical clades and 3
86 so called cryptic clades, that could be considered a separate genomospecies (Knight *et al.*, 2021). Epidemic
87 strains fall generally into clade 2 (RT027 and related strains) and clade 5 (RT078 and related strains). NTCD
88 have been reported in multiple clades, such as clade 1 (which includes RT010)(Baktash *et al.*, 2022), clade 4
89 (Imwattana *et al.*, 2020), clade C-I and clade C-II (Ducarmon *et al.*, 2023). Nevertheless, such strains are
90 generally understudied compared to the toxigenic counterparts.

91 There is epidemiological and experimental evidence that NTCD carriage is associated with lower
92 incidence of CDI, that NTCD colonization can prevent CDI disease and can reduce CDI recurrence in intestinal
93 models, animals and humans (Natarajan *et al.*, 2013, Gerding *et al.*, 2018, Etifa *et al.*, 2023). The strongest
94 evidence for use of NTCD as a therapeutic intervention is for strain M3 (a RT010 isolate) in humans (Villano *et*
95 *al.*, 2012, Gerding *et al.*, 2015, Sambol *et al.*, 2023) and strain Z31 (RT009) in piglets (Oliveira Junior *et al.*,
96 2019, Oliveira Junior *et al.*, 2019).

97 In addition to potential use as a live biotherapeutic product, NTCD could provide a chassis for
98 engineering of immune-epitopes and therefore serve as a potential vaccine (Hughes *et al.*, 2022, Wang *et al.*,
99 2022, Wang *et al.*, 2022), or be used to study aspects of CDI disease that are generally confounded by toxin-
100 mediated effects, such as early colonization events.

101 In light of the possible applications of NTCD, and the relative paucity of well-characterized NTCD
102 strains, we present here a detailed analysis of L-NTCD03, a clade 4 non-toxigenic *C. difficile* strain.
103
104
105 **Materials and Methods**
106
107 **Bacterial strains and growth conditions**
108 L-NTCD03 was isolated from fecal material of a healthy elderly subject negative for HIV-1, HIV-2, HCV, HBV, as
109 follows. Fecal material was stored in Stool Transport and Recovery (STAR) buffer and stored at -80C. Ethanol
110 treated material was inoculated into *C. difficile* enrichment modified broth (CDEB MOB; Mediaproducts NV,
111 Groningen, The Netherlands, cat no. 21.1295). After 6 days of growth at 37C under anaerobic conditions, the
112 culture was plated onto *C. difficile* selective growth medium (CLO; VWR International, cat.no. 43431). From
113 this medium, a colony was streaked to singles on a Tryptic Soy Sheep Blood medium (TSS; bioMérieux, cat.no.
114 43009,), and growth was harvested into glycerol-containing broth (Tritium Microbiology, cat. no. I200.36.0001)
115 for storage at -80°C.
116 Control strains belonging to PCR ribotype 027 (LL-027) and 078 (LL-078) were obtained from the
117 Leeds-Leiden collection (Knetsch *et al.*, 2012, Baktash *et al.*, 2022).
118 Strains were cultured in simulated ileal effluent medium (SIEM)(Minekus *et al.*, 1999, Wiese *et al.*,
119 2022), Brain-Heart Infusion (BHI) broth, BHI supplemented with yeast extract (BHI-Y; BHI with 0.5 % yeast
120 extract) or CDMN (Aspinall & Hutchinson, 1992) medium supplemented with 0.1% sodium taurocholate
121 (CDMNT).
122
123 **Molecular biology**
124 A genomic region including *cfr*(B) and its native promoter was amplified by PCR using Q5 polymerase (NEB)
125 and primers oIMM-01 and oIMM-02. The resulting PCR product was digested with KpnI and BamHI and cloned
126 into similarly digested pAP24 (Oliveira Paiva *et al.*, 2016). The resulting plasmid, pIMM03, was sequence
127 verified using primers NF793, NF794 (Fagan & Fairweather, 2011), oIMM-01, oIMM02, oIMM-03 and oIMM-04
128 was introduced using standard laboratory methods into strain 630Δ*erm* (van Eijk *et al.*, 2015, Roseboom *et al.*,
129 2023). Transconjugants were verified by PCR using primers oWKS-1070/oWKS-1071 (targeting chromosomal

130 *gluD*), oWKS-1387 and oWKS-1388 (targeting plasmid-located *traJ*) and oIMM-01/oIMM-02 (targeting *cfr*(B))
131 using appropriate controls. All oligonucleotide sequences are listed in **Table 3**.
132
133 **Antimicrobial susceptibility testing**
134 To determine minimal inhibitory concentrations (MIC) of a panel of antibiotics epsilometer tests
135 (Etests) were used. This panel consisted of cotrimoxazol, linezolid, metronidazole (Liofilchem), augmentin,
136 cefuroxime, ciprofloxacin, chloramphenicol, clindamycin, erythromycin, meropenem, moxifloxacin, penicillin,
137 rifampicin, tetracyclin, teicoplanin and vancomycin (bioMerieux). For this test, bacterial suspensions
138 corresponding to a turbidity of 1.0 McFarland unit were plated on Brucella blood agar supplemented with 5
139 mg L^{-1} hemin and 1 mg L^{-1} vitamin K (bioMerieux) plates, unless indicated otherwise. MIC values were
140 determined after 48 h of anaerobic incubation at 37°C as recommended by Clinical and Laboratory Standards
141 Institute (CLSI), including relevant control strains (CLSI, 2012). Fidaxomicin MIC was determined using the agar
142 dilution method according to CLSI guidelines on fresh Brucella Blood Agar supplemented with 5 mg L^{-1} hemin
143 and 1 mg L^{-1} vitamin K. Epidemiological cut-off values were used as defined by European Committee on
144 Antimicrobial Susceptibility Testing (EUCAST, 2026), when available.
145 MIC measurements for engineered strains (3 independent transconjugants) were performed on BHI-
146 yeast extract agar with either an E-test (clindamycin, linezolid) (bioMerieux or Liophilchem, respectively) or by
147 incorporating retapamulin (Sigma CDS023386) or streptogramin A/virginiamycin M1 (Sigma V2753) at 0-128
148 mg/L into the agar.
149
150 **PCR ribotyping**
151 Capillary gel electrophoresis ribotyping of L-NTCD03 was performed according to standardized protocols
152 (Fawley *et al.*, 2015). In short, 2µl of isolated DNA was added to 23 µl of the master mix which includes the 16S
153 and 23S primers and HotStart Taq Master Mix (Qiagen). Using a MyCycler thermocycler (Biorad), the resulting
154 DNA mix was subjected to an enzyme activation step at 95 °C for 15 minutes followed by 24 cycles of
155 amplification at 95 °C for 1 minute, 1 minute at 57 °C and 1 minute at 72 °C. Finally, the DNA mix was
156 subjected to 72 °C for 30 minutes. The sample was prepared for analysis by adding PCR product as 1 µl of PCR
157 product to 8.5 µl HiDi formamide (Applied Biosystems) and 0.5 µl of GeneScan™ 1200 LIZ marker (Thermo
158 Fisher) and samples was denatured at 95 °C for 5 minutes. To determine the ribotype, it was then analyzed

159 using the ABI3500XL (capillary length 50 cm) and the resulting *.fsa files were compared to a reference
160 database in BioNumerics (bioMérieux).
161
162 **Toxin ELISA**
163 To determine the productions of Toxin A and B, the *C. difficile* Tox A/B II™ kit (Techlab) was used according to
164 manufacturer's protocol with a minor modification. In short, the supernatants that were collected at 0, 24, 48,
165 72 and 96 h from growth curves in SIEM pH=5.8 and pH=6.8 were filtered using a UNIFILTER microplate device
166 (0.45 µm cellulose acetate filter, long drip, 96 wells, GE Health Care Life Sciences). The samples were applied to
167 the filter plate and centrifuged at 3220 G for 5 minutes at 4°C. The filtrates were used in the analysis as
168 described by manufacturer and the optical density was measured at 450 nm (OD_{450}). A threshold value of
169 OD_{450} of 0.12 was used determine whether toxins were present in the filtrate.
170
171 **Cell lines and culture conditions**
172 Human colorectal adenocarcinoma cells (Caco-2) were obtained from the American Type Culture Collection
173 (ATCC-HTB-37) and cultured in minimum essential medium (MEM, Gibco) supplemented with 10% bovine fetal
174 serum (10% FCS), 1% non-essential amino acids (NEAA, Lonza), 2 mM glutamine (Sigma Aldrich), 100 units/ml
175 penicillin (Sigma Aldrich), and 100 units/ml streptomycin (Sigma Aldrich). Epithelial-like, mucin-producing,
176 LS174T cells were obtained from Sigma Aldrich (87060401) and cultured in the medium described for Caco-2.
177 Both cells were grown to 80% confluency before experimental conditions were prepared.
178
179 ***In vitro* intestinal epithelial barrier model**
180 The apical side of Thincert 12 well cell culture inserts (PET, pore size 0.4 µm, Greiner Bio-one) were coated
181 with 250 µg/well purified human collagen type IV (OptiCol collagen Type IV, dissolved in 0.25% acetic acid, Cell
182 Guidance Systems) and washed with sterile PBS after 1-2 h incubation.
183 To mimic the human colon environment, an 80:20 ratio mixture of Caco-2 and LS174T in MEM
184 supplemented with 10% FCS, 1% non- NEAA, 2 mM glutamine, 100 U/ml penicillin, and 100 U/ml streptomycin
185 (cell culture medium) was prepared. To function as controls, 100:0 and 0:100 ratio mixtures of Caco-2 and
186 LS174T were prepared in cell culture medium. For all conditions, $1*10^5$ cells were seeded on the apical side of
187 the PET membrane. To mimic the intestinal environment, medium was present in both the basal compartment

188 (the well) and apical compartment (on top of the PET membrane) of the system. The systems were incubated
189 at 37°C and 5% CO2. The cells in this model were allowed to grow and differentiate for 21 days during which
190 the medium in both compartments was refreshed every other day.

191 To monitor the development of the *in vitro* intestinal epithelial barrier model, starting at T=0 the
192 transepithelial electrical resistance (TEER) values were measured using EVOM-2 resistance meter (World
193 Precision Instruments) every 7 days.

194 On day 21, the medium in the apical compartment of the system was replaced with a 10 times
195 diluted, in cell culture medium, supernatant harvested at 72 h in a growth curve of all of the strains in BHI-y
196 medium. This supernatant was incubated in the apical compartment for 1 hour at 37°C and 5% CO2, removed
197 afterwards and replaced with cell culture medium. In every condition, a control well was exposed to calcium
198 free medium (SMEM, Gibco) to determine as a positive control. TEER measurements were performed at 4
199 (only SMEM condition), 24, and 48 h post-exposure. Morphology was assessed under light microscopy every
200 24 hrs.

201

202 **Swine IsoLoop model**

203 We compared the effect of L-NTCD03 and LL-078 on intestinal mucosa *in vivo* in the pig IsoLoop model, a
204 translational surgical *in situ* ileal loop platform for host-microbiome-pathogen interface (Bayne *et al.*, 2025). 12
205 h before the start of the surgery, 1 ml was drawn from a culture in the exponential growth phase of either L-
206 NTCD-03 or LL-078 in BHI-y and inoculated into fresh, pre-reduced CDMNT medium and grown anaerobically at
207 37 °C. 10 ml of culture was aliquoted per loop and stored anaerobically at room temperature until injection
208 was required.

209 3-month-old, female pigs (*Sus scrofa*, mixed breed, 50-60kg) were used under USDA pain category D,
210 per Institutional Animal Care and Use Committee (IACUC) protocol IACUC-22-066 essentially as described
211 (Bayne *et al.*, 2025).

212 In short, the pig was placed in dorsal recumbency under general anesthesia. Ileal loops were rinsed
213 with sterile saline solution before treatment with an antibiotic cocktail (60 mg/L norfloxacin; 160 mg/L
214 moxalactam) for 30 minutes. After a saline rinse, each independent loop except for the most aboral segment
215 was inoculated using a tuberculin needle full thickness into the lumen. Upon recovery, animals were housed
216 under standard husbandry conditions with regular veterinary assessments to ensure welfare. The loops were

217 sampled at euthanasia by cutting the mesentery and immediately cooling the intestines on ice. On ice, the
218 loops were cut open one by one and a piece of tissue, including intestinal content, was fixed in 10% neutral
219 buffered formalin (VWR) before embedding in paraffin.

220 5µm-thick tissue sections were stained with hematoxylin and eosin. Microscopic analysis of
221 histopathologic features was conducted by a board-certified pathologist, blinded to sample identities. The
222 scoring rubric, including descriptive statistics applied, is provided as **Supplementary Information**, and raw data
223 of the scoring is included as **Supplementary Table 1**. Scores are reported as total histological score per ileal
224 loop (range 0-20), computed as the sum for four 0-5 ordinal components (epithelial necrosis, mucosal/lamina
225 propria edema, crypt abscess and neutrophils in villi/lamina propria). Statistical analyses of histological scores
226 were performed in Python (NumPy/SciPy); figures were generated with matplotlib. All tests were two sided
227 with $\alpha = 0.05$.

228

229 **DNA extraction and genome sequencing**

230 To extract pure high-molecular weight total DNA, a two-fold serial dilution of L-NTCD03 in BHI-Y medium was
231 prepared. After overnight incubation at 37°C in an anaerobic environment, 4mL of culture with an optical
232 density at 600nM between 0.6 and 0.8 was spun down and DNA was extracted from the cell pellet using the
233 500/G genomic tip kit (Qiagen), according to the instructions of the manufacturer. Quantity and quality of the
234 DNA was verified by gel electrophoresis on a 0.8% agarose gel, using the Qubit dsDNA high-sensitivity kit
235 (Qubit) and a Femto Pulse system (Agilent), according to the manufacturer's protocols.

236 PacBio sequencing libraries were generated according to the manufacturer's multiplexed microbial
237 library preparation protocol, part number 101-696-100, version 7, July 2020 release (Pacific Biosciences) using
238 the SMRTbell Express Template Prep Kit v2.0 with the following modifications: genomic DNA was sheared
239 using Speed 34 on the Megaruptor 3 (Diagenode) and an additional size selection step of 6-50kb fragments on
240 the Blue Pippin (Sage Science) was included for the final SMRT bell library. The libraries were sequenced on a
241 Sequel II platform (Pacific Biosciences) using the Sequel II Binding Kit v2.0, Sequencing Primer v4, Sequencing
242 Kit v2.0 and a 30hr movie time.

243

244 **Genome annotation and bioinformatics analyses**

245 De novo genome assembly was carried out using Hifiasm (version 0.16.1-r375; parameters '--hg-size 4m')
246 (Cheng *et al.*, 2021) and the start position was set to *dnaA* using Circlator fixstart (version 1.5.5 using default
247 parameters) (Hunt *et al.*, 2015). Completeness check was performed using Busco (version 5.2.2; parameters '-
248 m genome -l clostridia_odb10') (Manni *et al.*, 2021) and assembly statistics were calculated and visualised with
249 Quast (version 5.0.2; using NZ_CP076401 as reference genome)(Gurevich *et al.*, 2013). Finally, Prokka (version
250 1.14.6; parameters '--genus Clostridioides --species difficile --compliant')(Seemann, 2014) was used to
251 annotate the genome.

252 A database of AMR genes was constructed using the AMRFinder plus tool v3.10.23 (parameters "-n"
253 "–organism Clostridioides difficile", "—plus") to identify antimicrobial resistance (AMR) genes (Feldgarden *et*
254 *al.*, 2021). Minimal "% coverage of reference sequence" and "% Identity to refence sequence" were set to 60%
255 and 90% percent, respectively.

256 BacAnt (Hua *et al.*, 2021) and MobileElementFinder (Johansson *et al.*, 2021) were used to identify
257 putative transposable elements. progressiveMauve was used to align genome sequences (Darling *et al.*, 2010).

258 Multi-locus sequence typing (MLST) was performed using mlst (v2.19.0) with the PubMLST *C. difficile*
259 database updated to October 21, 2021, (Jolley *et al.*, 2018) and verified on December 1, 2025.

260 Genomic comparisons were made in Geneious R10 (BioMatters Ltd), and figures for publication were
261 prepared using CAGECAT (van den Belt *et al.*, 2023) and Adobe Illustrator 26.3.1.

262

263 **Data availability**

264 L-NTCD03 genome information is available under BioProject PRJEB62683 (raw reads: ERR11495271, assembly:
265 ERZ18456945). The annotated genome is OX637968.1.

266

267

268 **Results**

269

270 **L-NTCD03 belongs to a rare PCR ribotype, RT416**

271 As part of a study investigating carriage of multidrug resistant organisms and *C. difficile* in nursing homes
272 (Ducarmon *et al.*, 2021), fecal material was obtained from a healthy elderly subject. *C. difficile* was cultured
273 from this material as described in Materials and Methods. The resulting isolate was negative in a multiplex PCR
274 that targets the toxin genes *tcdA*, *tcdB, cdtA* and *cdtB* (Control, 2018), suggesting that the isolate was non-
275 toxigenic. Hereafter, the isolate is referred to as L-NTCD03.
276 We performed capillary electrophoresis PCR ribotyping (Fawley *et al.*, 2015) of L-NTCD03 through the
277 Dutch Expertise Center for *C. difficile*, hosted at the LUMC. We initially failed to obtain a ribotype assignment,
278 as the banding pattern was not present in our database. The *.fsa files were shared with the *Clostridioides*
279 *difficile* Ribotyping Network Laboratory (CDRN; PHE Microbiology Services, Leeds, UK), and they determined
280 the isolate to belong to PCR ribotype 416. Since this identification, no other isolates were identified with the
281 same ribotype in the Dutch National Expertise Center for *C. difficile* infections. This suggests a prevalence in
282 the Netherlands that is below 0.01% on the basis of the number of strains typed since then.
283
284 **L-NTCD03 is susceptible to clinically used antimicrobials**
285 To determine whether L-NTCD03 the minimal inhibitory concentration for different antimicrobials, we
286 performed antimicrobial susceptibility testing using agar dilution (for fidaxomicin) or Etest (augmentin,
287 cefuroxime, chloramphenicol, clindamycin, cotrimoxazol, erythromycin, linezolid, metronidazole, meropenem,
288 moxifloxacin, penicillin, rifampicin, tetracyclin, teicoplanin and vancomycin) methods on Brucella Blood Agar
289 (BBA), as recommended by CLSI (CLSI, 2012). Out of the 17 antimicrobials tested, L-NTCD03 demonstrated
290 elevated MICs for cefuroxime, chloramphenicol, ciprofloxacin, erythromycin, linezolid, rifampicin and
291 tetracycline (**Table 1**). In contrast, the strain is susceptible to antimicrobials that are used in CDI therapy -
292 fidaxomicin, vancomycin and metronidazole – as well as several others (**Table 1**). As BBA is a suboptimal
293 medium for determining resistance to metronidazole, we also retested the isolate on recently recommended
294 Fastidious Anaerobe Agar supplemented with horse blood (Freeman *et al.*, 2025); this confirmed susceptibility
295 to metronidazole (data not shown). These results demonstrate that L-NTCD03 would likely be suppressed or
296 eradicated using standard antimicrobial therapy for CDI, but not by certain other antimicrobials that increase
297 susceptibility for CDI.
298
299 **Supernatant from L-NTCD03 does not contain detectable toxin A and B**

300 To confirm the absence of toxins, as suggested by the multiplex PCR result, we assessed the presence of TcdA
301 and TcdB in culture supernatant using an enzyme-coupled immune assay (Techlab). We used a medium that
302 mimicks the physiological conditions in the gut: simulated ileal effluent medium, SIEM (Minekus *et al.*, 1999,
303 Wiese *et al.*, 2022).
304 During 96 h of growth in SIEM, toxin levels were below the limit of detection for all supernatants
305 derived from L-NTCD03, as well as for the reference non-toxigenic strain LL-010 (**Figure 1A**). In contrast, toxins
306 were readily detected in culture supernatants derived from the toxigenic reference strains LL-027 and LL-078
307 (**Figure 1A**).
308
309 **Supernatant from L-NTCD03 does not affect transepithelial electrical resistance**
310 Though our results clearly indicate the absence of TcdA and TcdB, we considered that there could be other
311 factors that affect epithelial integrity, not detected in our assays so far. For this reason, we assessed the effect
312 of culture supernatant derived from L-NTCD03, LL-010, LL-027 and LL-078 in an *in vitro* model for epithelial
313 integrity. In this model, a mixture of Caco2 and mucin-producing LS174T cells is grown in a transwell system
314 and the transepithelial electrical resistance (TEER), a proxy for epithelial integrity, is measured using
315 electrodes.
316 The TEER values gradually increased over the first 14 days of incubation, consistent with cells growing
317 to confluency, and stabilized between days 14 and 21 (**Figure 1B**). When filtered supernatants from 72h-
318 cultures in BHI were applied to the cell layer, no drop in TEER was observed for the non-toxigenic strains (LL-10
319 and L-NTCD03), whereas LL-027 and LL-078 derived supernatants resulted in a significant decrease (**Figure 1B**).
320 Similar results were obtained when only LS174T cells or Caco2 cells were used (data not shown). This shows
321 that no other factors are produced by the non-toxigenic *C. difficile* strains that affect TEER in this cellular
322 model.
323
324 **L-NTCD03 grows similar to other isolates in a simulated ileal effluent medium**
325 To assess the growth and sporulation of L-NTCD03 in relation to well-characterized common subtypes of *C.*
326 *difficile* in SIEM, we monitored the total number of colony forming units (CFU) per milliliter (mL) over a period
327 of 14 days. Spore formation was monitored by enumeration of ethanol resistant CFUs.
328 Growth of L-NTCD03 was indistinguishable from LL-010, LL-027 and LL-078 for the first 6 h, during

329 which the number of CFU/mL increased ~3 log (**Figure 1C**). During stationary phase, we observed a lower total
330 cell count of ~10^7 CFU/mL, for all strains (**Figure 1C**).
331 No spore production was found during the first 6h of growth in SIEM (**Figure 1D**). For LL-010 and LL-
332 027 spores were detectable at 24h, but for L-NTCD03 and LL-078 spores were first found at the 48h-timepoint.
333 Beyond this point, sporulation dynamics were comparable between all strains **Figure 1D**).
334 Thus, under the conditions tested, L-NTCD03 shows robust growth and sporulation, in line with other
335 *C. difficile* strains.
336
337 **Phenotype microarrays show a common carbon utilization profile for L-NTCD03**
338 In order to assess the carbon utilization by L-NTCD03 we performed phenotype microarrays on Biolog PM1 and
339 PM2 plates, and analyzed the results using AMIGA software, as described previously (Midani *et al.*, 2021). We
340 used an arbitrary cut-off of 1.5-fold increase in or a 2-fold decrease in optical density to define differential
341 growth. We observed stimulated growth on the carbon sources N-Acetyl-D-Glucosamine, D-Mannose, D-
342 Mannitol, D-Fructose, alpha-D-Glucose, N-AcetylNeuraminic Acid, D-Melezitose, D-Tagatose and D-
343 Glucosamine (**Supplemental Table S1**). A decreased cell density was observed in the presence of Glyoxylic Acid
344 and Glycyl-LGlutamic Acid (**Supplemental Table S1**).
345 In parallel experiments, we observed similar profiles for representative strains from PCR ribotype 010,
346 027 and 078 (data not shown)(Collins *et al.*, 2018, Midani *et al.*, 2025). We conclude that L-NTCD03 carbon
347 utilization is similar to that of other *C. difficile* isolates.
348
349 **L-NTCD03 does not induce *C. difficile*-associated intestinal lesions in the swine IsoLoop model**
350 We have previously demonstrated the utility of the swine IsoLoop model for assessing *C. difficile*–associated
351 lesions in a translationally relevant gut microbiota–pathogen interface (Bayne *et al.*, 2025). Using this platform,
352 we compared the effects of L-NTCD03 in relation to the effects induced by the toxigenic reference strain LL-
353 078.
354 We inoculated multiple loops in the same animal (one animal per strain, either LL-078 or L-NTCD03),
355 and compared the histology to control loops without *C. difficile* and normal ileum (**Figure 2)**. Loops inoculated
356 with LL-078 showed signs of inflammation, whereas those inoculated with L-NTCD03 were comparable to the
357 control loop (**Figure 2A**). The total histological score (further detailed in the Methods section of this

358 manuscript) of samples derived from loops inoculated with LL-078 were significantly higher than those derived
359 from , whereas the histology of L-NTCD03 derived samples was comparable to that of control loops (**Figure 2B**
360 and **Supplemental Table 1**).
361
362 **L-NTCD03 is an ST39 (clade 4) isolate carrying a *cfr*(B) resistance gene**
363 *C. difficile* is a phylogenetically diverse species, with isolates falling into at least 5 classical (CDI-associated)
364 clades and 3 so called cryptic clades, that have been proposed to form separate genomospecies (Knight *et al.*,
365 2021). To place the L-NTCD03 in phylogenetic context, we reconstructed the complete genome sequence of
366 the strain using Pacific Biosciences circular consensus sequencing (BioProject PRJEB62683). After assembly, the
367 resulting genome showed a single circular contig of 4,318,385 bp – indicating the absence of
368 extrachromosomal elements - and an average [G+C]-content of 28,91%. Reference assembly of short-read
369 (Illumina) sequence data did not identify any nucleotide variants (data not shown), underscoring the quality of
370 the assembly.
371 We derived the 7-gene multilocus sequence type of our isolate using PubMLST (Griffiths *et al.*, 2010,
372 Jolley *et al.*, 2018). L-NTCD03 was found to belong to ST39 (*adk* 3, *atpA* 7, *dxr* 10, *glyA* 8, *recA* 7, *sodA* 2, *tpi*
373 10), which falls into clade 4. A core genome phylogenetic tree of representative isolates of different *C. difficile*
374 clades using Panaroo and IQTree confirmed this placement (data not shown)(Minh *et al.*, 2020, Tonkin-Hill *et*
375 *al.*, 2020, Baktash *et al.*, 2022).
376 We performed automated annotation of the genome sequence using Prokka (Seemann, 2014). This
377 resulted in 3,844 predicted coding sequences, 88 tRNAs, 34 rRNAs, 1 tmRNA and 8 repeat regions. As
378 expected, no complete genes corresponding to the toxin genes *tcdA*, *tcdB*, *cdtA* and *cdtB* were detected; in
379 stead the PaLoc insertion site conforms to what has been described for clade 4 strains (115bp insertion)(Dingle
380 *et al.*, 2014).
381 We used AMRfinderPlus to identify antimicrobial resistance genes in the L-NTCD03 genome
382 (Feldgarden *et al.*, 2022). We found 14 putative antimicrobial resistance genes, which are associated with 12
383 different classes of antibiotics (**Supplemental Table 2**); ten of these might be linked to the phenotypically
384 observed reduced susceptibility/resistance (**Table 1**).
385 Though *cfr*(B) has been implicated in antimicrobial resistance of *C. difficile* to PhLOPSa (phenicol,
386 lincosamide, oxaxolidinone, pleuromutilin and streptogramin A) antimicrobials (Marin *et al.*, 2015, Stojkovic *et*

387 *al.*, 2019), a direct causal role for this gene in resistance to these antimicrobials has not been shown to date.
388 Therefore, we cloned the *cfr*(B) gene under its native promoter in a shuttle plasmid and introduced this
389 plasmid into the commonly used *C. difficile* laboratory strain 630Δ*erm* (Hussain, 2005, van Eijk *et al.*, 2015). We
390 assessed antimicrobial susceptibility using Etest and found that introduction of *cfr*(B) increased the minimal
391 inhibitory concentration for clindamycin, linezolid, retapamulin and streptogramin A (**Table 2**) in comparison
392 to a control strain carrying a similar plasmid that carried the reporter gene *sluc*^{opt} (Oliveira Paiva *et al.*, 2016)
393 rather than *cfr*(B). The MIC increased >128-fold for clindamycin (from 2 mg/L to >256 mg/L), 12-fold for
394 linezolid (from 1 mg/L to 12 mg/L), 64-fold for retapamulin (from 0.125 mg/L to 16 mg/L) and 8-fold for
395 streptogramin A (from 2 mg/L to 16 mg/L) in the presence of *cfr*(B). We observed no change in MIC for
396 vancomycin and metronidazole (data not shown). This result indicates that *cfr*(B) can indeed confer resistance
397 to lincosamide, oxazolidinone, pleuromutilin and streptogramin antimicrobials in *C. difficile*, consistent with
398 expectations (Marin *et al.*, 2015, Stojkovic *et al.*, 2019).
399
400 **The genome of L-NTCD03 harbors several putative mobile genetic elements**
401 The BacAnt annotation server (Hua *et al.*, 2021) identified two putative transposable elements, with homology
402 to Tn*4451* (GenBank U15027; 94.57% identity and 100% coverage; bp 524023-530368) and Tn*5405* (GenBank
403 U73027; 99.84% identity and 95.97% coverage; bp 551080-553654). Of note, the *catP* gene is contained on the
404 former, suggesting a potential for transmission of this resistance determinant. MobileElementFinder
405 (Johansson *et al.*, 2021), in addition to Tn*4551*, identifies a chromosomal region with homology to Tn*6009*
406 (GenBank EU399632; identity 99.95% and coverage 100%; bp 268640-270528). Comparison with a closely
407 related clade 4 genome (DSM 29629, GenBank NZ_CP016104) reveals that this is in fact a 17.9-kb transposon
408 highly similar to Tn*916*, which has inserted in a gene (*pdeR*) encoding a GGDEF domain containing protein (in L-
409 NTCD03 this gene is split into two ORFs: LLHAOGBK_00311 and LLHAOGBK_00328) (**Figure 3**). The transposon
410 (**GenBank OR192611**) is also found in several *Streptococcus* and *Enterococcus* genome assemblies (data not
411 shown), and was assigned the number Tn*7696* by the transposon registry (Tansirichaiya *et al.*, 2019).
412 Compared to Tn*916*, Tn*7696* has a 120-bp in-frame deletion in the gene encoding a putative endopeptidase
413 p60 precursor (ORF14 in Tn*916*, LLHAOGBK_00319 in L-NTCD03) as well as several SNPs.
414 Finally, we employed two tools to predict i) putative phages (Wishart *et al.*, 2023) and ii) genomic
415 islands (Bertelli *et al.*, 2017). This identified two possible complete (pro)phages in L-NTCD03, with homology to

416 phiCDHM19 (NC_028996; bp 664975-719994) and phiC2 (NC_09231; bps 2626715-2687566) both of which are
417 also predicted with high confidence by geNomad (Camargo *et al.*, 2024), and 2 large (bp 490582-569665 and
418 3900143-3992891) plus several small regions that are likely horizontally acquired.
419 Overall, the complete genome sequence suggests a clear relation with other clade 4 *C. difficile*
420 isolates, and a significant contribution of horizontal gene transfer to its genetic content.
421
422
423 **Discussion**
424
425 Here, we provided a characterization of L-NTCD03, isolated from a healthy elderly subject. We confirmed that
426 this isolate does not express the large clostridial toxins *tcdA* and *tcdB*, using ELISA, and showed that
427 supernatants derived from an L-NTCD03 culture do not induce a loss of TEER in a trans-well model of colonic
428 epithelium. Additionally, data from the swine IsoLoop model suggest that there is no induced pathology in
429 loops inoculated with L-NTCD03 compared to controls. The loop experiment provides insight into strain
430 behavior within a translationally relevant, *C. difficile*–predisposing intestinal environment, using a customized
431 dysbiotic gut segment that enables precise local control of the bacterial inoculum, bile acid milieu, and other
432 key microenvironmental parameters. The data is in line with the genomic analysis, which shows a lack of
433 identifiable toxin genes, including the binary toxin locus. Together, these data strongly suggest that L-NTCD03
434 is unlikely to induce disease.
435 The high-quality complete genome generated for L-NTCD03 as part of this work, allowed us to place
436 the PCR ribotype 416 strain in clade 4. The most closely related publicly available genome at the time of
437 analysis is DSM 29629 (Riedel *et al.*, 2017)(CP016104.1). Like L-NTCD03, this strain was non-toxigenic and
438 assigned to clade 4, however, it is listed as ribotype SLO 235. At present it is unknown if the ribotyping
439 patterns for SLO 235 and RT416 (as determined by capillary ribotyping and assigned at the CDRN) are similar or
440 the same. Interestingly, in the manuscript describing DSM 29629 the authors note metabolic versatility
441 between 17 different *C. difficile* strains that does not appear to necessarily follow the 5 major phylogenetic
442 clades (clade) or PCR ribotypes tested. In the present work, we find that L-NTCD03 demonstrated a carbon
443 utilization profile that is quite similar to that of other *C. difficile* strains under the conditions tested. We have
444 to note that this was assessed at a single concentration and we cannot rule out that differences may exists at

445 alternative concentrations, similar to what has been noted for other *C. difficile* strains belonging to other
446 ribotypes (Collins *et al.*, 2018, Midani *et al.*, 2025).

447 We have determined the phenotypic antimicrobial resistance profile for 17 antimicrobials and found
448 that several could be explained by genetic determinants identified in the complete genome of L-NTCD03.
449 Some of these determinants appear to be associated with mobile genetic elements (Bannam *et al.*, 1995,
450 Derbise *et al.*, 1997, Soge *et al.*, 2008, Hua *et al.*, 2021), supporting the view that NTCD strains may act as a
451 reservoir for resistance determinants (Imwattana *et al.*, 2020). As observed also by others for NTCD strains
452 (Imwattana *et al.*, 2020), we also observed resistance to rifampicin and ciprofloxacin in L-NTCD03. It is
453 interesting to speculate that high levels of resistance in NTCD may relate to prolonged carriage, or reflect
454 antibiotic use in geographic areas where these strains are common. Rifampicin, for instance, is commonly used
455 in the treatment of tuberculosis patients. For clade 4 strains, high prevalence in Asia has been noted
456 (Imwattana *et al.*, 2020) but such strains are also more broadly found (Viprey *et al.*, 2022). Notably, though the
457 *nimB*-Cd resistance gene was identified (**Supplemental Table 2**), we observed no resistance to metronidazole.
458 Consistent with this, *nimB* is commonly found in susceptible isolates of *C. difficile* and L-NTCD03 lacks the
459 P*nimB*^{G} mutation associated with increased *nimB* expression and inducible metronidazole resistance (Olaitan
460 *et al.*, 2023). It also highlights the putative nature of automated identification of antimicrobial resistance
461 determinants.

462 Finally, we identified the *cfr*(B) gene in L-NTCD03. The *cfrB* gene encodes a rRNA methyltransferase
463 that confers multidrug resistance by ribosomal target modification and, in addition to *C. difficile*, has been
464 found in *Enterococcus* spp and methicillin-resistant *Staphylococcus aureus*. We showed that this gene can
465 confer resistance to clindamycin (>256 mg/L), linezolid (12 mg/L), repatamulin (16 mg/L) and streptogramin A
466 (16 mg/L) in the RT012 laboratory strain 630Δ*erm* (van Eijk *et al.*, 2015). Our data confirm that *cfr*(B) is a
467 legitimate PhLOPSa (phenicol, lincosamide, oxazolidinone, pleuromutilin, streptogramin A) resistance gene.
468 We were unable to establish whether *cfr*(B) plays a role in phenicol resistance, though, as L-NTCD03 also
469 contains the *catP* (chloramphenicol resistance gene) and the plasmid we used to introduce the *cfr*(B) gene in
470 our laboratory strain also carries a *catP* resistance determinant (Fagan & Fairweather, 2011, Oliveira Paiva *et*
471 *al.*, 2016). We have, however, independently observed that *catP*-negative clinical isolates that carry *cfr*(B)
472 demonstrate elevated chloramphenicol MICs compared to isolates that lack *cfr*(B), suggesting that *cfr*(B) also
473 affects chloramphenicol MICs. Though it has previously been shown that *cfr* gene carriage can be associated

with linezolid resistance in *C. difficile* (Marin *et al.*, 2015, Stojkovic *et al.*, 2019) or lead to an increase in MIC for certain antibiotics when expressed in a heterologous host (Hansen & Vester, 2015), to our knowledge, the present study is the first direct demonstration of this function for *cfr*(B) as a PhLOPSa resistance gene in this organism.

Acknowledgements

We thank members of our laboratory as well as prof. dr. A.P. Roberts and prof. dr. L.C. Fortier for helpful discussions. We are indebted to prof. dr. P. Hiemstra and his team at LUMC for support with the TEER measurements and the CDRN (prof. M.H. Wilcox and dr. W. Fawley) for the ribotype assignment for this strain.

Funding

This work was supported, in part, by FEMS Research and Training Grant FEMSO-GO-2021-042 to BN.

Declaration of interest statements

The authors declare that the research was conducted in the absence of any commercial or financial relationships that could be construed as a potential conflict of interest.

Author contributions

BN, EJK and WKS conceived the study. CH and IMJGS performed typing and susceptibility testing, BN performed characterization of L-NTCD03 in *in vitro* and cellular assays. RHAMV and SLK performed PacBio sequencing. SN and QRD performed bioinformatics analyses. CKB and RAB performed the Biolog experiments. JB, CC, MLM, AL, BS and SM conducted the animal experiments. FY performed the histological scoring. EB, SM and TO reviewed the histology. WKS, TO, SM and EJK supervised work. BN and WKS drafted the manuscript. All authors edited the manuscript and agreed to its submission.

502 **References**

503 Aktories K, Schwan C & Jank T (2017) Clostridium difficile Toxin Biology. *Annu Rev Microbiol* **71**: 281-307.
504 Aspinall ST & Hutchinson DN (1992) New selective medium for isolating Clostridium difficile from faeces. *J Clin*
505 *Pathol* **45**: 812-814.
506 Baktash A, Corver J, Harmanus C*, et al.* (2022) Comparison of Whole-Genome Sequence-Based Methods and
507 PCR Ribotyping for Subtyping of Clostridioides difficile. *J Clin Microbiol* **60**: e0173721.
508 Bannam TL, Crellin PK & Rood JI (1995) Molecular genetics of the chloramphenicol-resistance transposon
509 Tn4451 from Clostridium perfringens: the TnpX site-specific recombinase excises a circular transposon
510 molecule. *Mol Microbiol* **16**: 535-551.
511 Bayne J, Charavaryamath C, Hu Y*, et al.* (2025) The swine IsoLoop model of the gut host-microbiota interface
512 enables intra-animal treatment comparisons to advance 3R principles. *Gut Microbes* **17**: 2568706.
513 Bertelli C, Laird MR, Williams KP, Simon Fraser University Research Computing G, Lau BY, Hoad G, Winsor GL &
514 Brinkman FSL (2017) IslandViewer 4: expanded prediction of genomic islands for larger-scale datasets. *Nucleic*
515 *Acids Res* **45**: W30-W35.
516 Boekhoud IM, Hornung BVH, Sevilla E, Harmanus C, Bos-Sanders I, Terveer EM, Bolea R, Corver J, Kuijper EJ &
517 Smits WK (2020) Plasmid-mediated metronidazole resistance in Clostridioides difficile. *Nat Commun* **11**: 598.
518 Boekhoud IM, Sidorov I, Nooij S*, et al.* (2021) Haem is crucial for medium-dependent metronidazole resistance
519 in clinical isolates of Clostridioides difficile. *J Antimicrob Chemother* **76**: 1731-1740.
520 Braun V, Hundsberger T, Leukel P, Sauerborn M & von Eichel-Streiber C (1996) Definition of the single
521 integration site of the pathogenicity locus in Clostridium difficile. *Gene* **181**: 29-38.
522 Camargo AP, Roux S, Schulz F, Babinski M, Xu Y, Hu B, Chain PSG, Nayfach S & Kyrpides NC (2024) Identification
523 of mobile genetic elements with geNomad. *Nat Biotechnol* **42**: 1303-1312.
524 Cheng H, Concepcion GT, Feng X, Zhang H & Li H (2021) Haplotype-resolved de novo assembly using phased
525 assembly graphs with hifiasm. *Nat Methods* **18**: 170-175.
526 CLSI (2012) Methods for Antimicrobial Susceptibility Testing of Anaerobic Bacteria; Approved Standard - Eighth
527 edition. p.^pp. 56. Clinical and Laboratory Standards Institute, Wayne, PA.
528 Collins J, Robinson C, Danhof H, Knetsch CW, van Leeuwen HC, Lawley TD, Auchtung JM & Britton RA (2018)
529 Dietary trehalose enhances virulence of epidemic Clostridium difficile. *Nature* **553**: 291-294.
530 Control ECfDPa (2018) Laboratory procedures for diagnosis and typing of human Clostridium difficile infection.
531 p.^pp. Stockholm.
532 Crobach MJT, Vernon JJ, Loo VG, Kong LY, Pechine S, Wilcox MH & Kuijper EJ (2018) Understanding Clostridium
533 difficile Colonization. *Clin Microbiol Rev* **31**.
534 Darling AE, Mau B & Perna NT (2010) progressiveMauve: multiple genome alignment with gene gain, loss and
535 rearrangement. *PLoS One* **5**: e11147.
536 Derbise A, de Cespedes G & el Solh N (1997) Nucleotide sequence of the Staphylococcus aureus transposon,
537 Tn5405, carrying aminoglycosides resistance genes. *J Basic Microbiol* **37**: 379-384.
538 Dingle KE, Elliott B, Robinson E*, et al.* (2014) Evolutionary history of the Clostridium difficile pathogenicity
539 locus. *Genome Biol Evol* **6**: 36-52.
540 Ducarmon QR, van der Bruggen T, Harmanus C, Sanders I, Daenen LGM, Fluit AC, Vossen R, Kloet SL, Kuijper EJ
541 & Smits WK (2023) Clostridioides difficile infection with isolates of cryptic clade C-II: a genomic analysis of
542 polymerase chain reaction ribotype 151. *Clin Microbiol Infect* **29**: 538 e531-538 e536.
543 Ducarmon QR, Terveer EM, Nooij S*, et al.* (2021) Microbiota-associated risk factors for asymptomatic gut
544 colonisation with multi-drug-resistant organisms in a Dutch nursing home. *Genome Med* **13**: 54.
545 Etifa P, Rodriguez C, Harmanus C*, et al.* (2023) Non-Toxigenic Clostridioides difficile Strain E4 (NTCD-E4)
546 Prevents Establishment of Primary C. difficile Infection by Epidemic PCR Ribotype 027 in an In Vitro Human Gut
547 Model. *Antibiotics (Basel)* **12**.
548 EUCAST (2026) European Committee on Antimicrobial Susceptibility Testing. . p.^pp.
549 Fagan RP & Fairweather NF (2011) Clostridium difficile has two parallel and essential Sec secretion systems. *J*
550 *Biol Chem* **286**: 27483-27493.
551 Fawley WN, Knetsch CW, MacCannell DR, Harmanus C, Du T, Mulvey MR, Paulick A, Anderson L, Kuijper EJ &
552 Wilcox MH (2015) Development and validation of an internationally-standardized, high-resolution capillary gel-
553 based electrophoresis PCR-ribotyping protocol for Clostridium difficile. *PLoS One* **10**: e0118150.
554 Feldgarden M, Brover V, Fedorov B, Haft DH, Prasad AB & Klimke W (2022) Curation of the AMRFinderPlus
555 databases: applications, functionality and impact. *Microb Genom* **8**.

Feldgarden M, Brover V, Gonzalez-Escalona N*, et al.* (2021) AMRFinderPlus and the Reference Gene Catalog facilitate examination of the genomic links among antimicrobial resistance, stress response, and virulence. *Sci Rep* **11**: 12728.

Ferretti P, Wirbel J, Maistrenko OM*, et al.* (2023) C. difficile may be overdiagnosed in adults and is a prevalent commensal in infants. *bioRxiv* 2022.2002.2016.480740.

Freeman J, Sanders I, Harmanus C, Clark EV, Berry AM & Smits WK (2025) Antimicrobial susceptibility testing of Clostridioides difficile: a dual-site study of three different media and three therapeutic antimicrobials. *Clin Microbiol Infect* **31**: 1011-1017.

Gerding DN, Sambol SP & Johnson S (2018) Non-toxigenic Clostridioides (Formerly Clostridium) difficile for Prevention of C. difficile Infection: From Bench to Bedside Back to Bench and Back to Bedside. *Front Microbiol* **9**: 1700.

Gerding DN, Meyer T, Lee C*, et al.* (2015) Administration of spores of nontoxigenic Clostridium difficile strain M3 for prevention of recurrent C. difficile infection: a randomized clinical trial. *JAMA* **313**: 1719-1727.

Goorhuis A, Bakker D, Corver J, Debast SB, Harmanus C, Notermans DW, Bergwerff AA, Dekker FW & Kuijper EJ (2008) Emergence of Clostridium difficile infection due to a new hypervirulent strain, polymerase chain reaction ribotype 078. *Clin Infect Dis* **47**: 1162-1170.

Griffiths D, Fawley W, Kachrimanidou M*, et al.* (2010) Multilocus sequence typing of Clostridium difficile. *J Clin Microbiol* **48**: 770-778.

Gurevich A, Saveliev V, Vyahhi N & Tesler G (2013) QUAST: quality assessment tool for genome assemblies. *Bioinformatics* **29**: 1072-1075.

Hansen LH & Vester B (2015) A cfr-like gene from Clostridium difficile confers multiple antibiotic resistance by the same mechanism as the cfr gene. *Antimicrob Agents Chemother* **59**: 5841-5843.

He M, Miyajima F, Roberts P*, et al.* (2013) Emergence and global spread of epidemic healthcare-associated Clostridium difficile. *Nat Genet* **45**: 109-113.

Hua X, Liang Q, Deng M*, et al.* (2021) BacAnt: A Combination Annotation Server for Bacterial DNA Sequences to Identify Antibiotic Resistance Genes, Integrons, and Transposable Elements. *Front Microbiol* **12**: 649969.

Hughes J, Aston C, Kelly ML & Griffin R (2022) Towards Development of a Non-Toxigenic Clostridioides difficile Oral Spore Vaccine against Toxigenic C. difficile. *Pharmaceutics* **14**.

Hunt M, Silva ND, Otto TD, Parkhill J, Keane JA & Harris SR (2015) Circlator: automated circularization of genome assemblies using long sequencing reads. *Genome Biol* **16**: 294.

Hussain HA (2005) Generation of an erythromycin-sensitive derivative of Clostridium difficile strain 630 (630 erm) and demonstration that the conjugative transposon Tn916 E enters the genome of this strain at multiple sites. *Journal of Medical Microbiology* **54**: 137-141.

Imwattana K, Kiratisin P, Riley TV & Knight DR (2020) Genomic basis of antimicrobial resistance in non-toxigenic Clostridium difficile in Southeast Asia. *Anaerobe* **66**: 102290.

Johansson MHK, Bortolaia V, Tansirichaiya S, Aarestrup FM, Roberts AP & Petersen TN (2021) Detection of mobile genetic elements associated with antibiotic resistance in Salmonella enterica using a newly developed web tool: MobileElementFinder. *J Antimicrob Chemother* **76**: 101-109.

Jolley KA, Bray JE & Maiden MCJ (2018) Open-access bacterial population genomics: BIGSdb software, the PubMLST.org website and their applications. *Wellcome Open Res* **3**: 124.

Knetsch CW, Terveer EM, Lauber C, Gorbalenya AE, Harmanus C, Kuijper EJ, Corver J & van Leeuwen HC (2012) Comparative analysis of an expanded Clostridium difficile reference strain collection reveals genetic diversity and evolution through six lineages. *Infect Genet Evol* **12**: 1577-1585.

Knight DR, Imwattana K, Kullin B, Guerrero-Araya E, Paredes-Sabja D, Didelot X, Dingle KE, Eyre DW, Rodriguez C & Riley TV (2021) Major genetic discontinuity and novel toxigenic species in Clostridioides difficile taxonomy. *Elife* **10**.

Kordus SL, Thomas AK & Lacy DB (2022) Clostridioides difficile toxins: mechanisms of action and antitoxin therapeutics. *Nat Rev Microbiol* **20**: 285-298.

Leffler DA & Lamont JT (2015) Clostridium difficile infection. *N Engl J Med* **372**: 1539-1548.

Lim SC, Knight DR & Riley TV (2020) Clostridium difficile and One Health. *Clin Microbiol Infect* **26**: 857-863.

Mani J, Levy S, Angelova A, Hazrati S, Fassnacht R, Subramanian P, Richards T, Niederhuber JE, Maxwell GL & Hourigan SK (2023) Epidemiological and microbiome associations of Clostridioides difficile carriage in infancy and early childhood. *Gut Microbes* **15**: 2203969.

Manni M, Berkeley MR, Seppey M & Zdobnov EM (2021) BUSCO: Assessing Genomic Data Quality and Beyond. *Curr Protoc* **1**: e323.

Marin M, Martin A, Alcala L, Cercenado E, Iglesias C, Reigadas E & Bouza E (2015) Clostridium difficile isolates with high linezolid MICs harbor the multiresistance gene cfr. *Antimicrob Agents Chemother* **59**: 586-589.

Midani FS, Collins J & Britton RA (2021) AMiGA: Software for Automated Analysis of Microbial Growth Assays. *mSystems* **6**: e0050821.
Midani FS, Danhof HA, Mathew N, Ardis CK, Garey KW, Spinler JK & Britton RA (2025) Emerging Clostridioides difficile ribotypes have divergent metabolic phenotypes. *mSystems* **10**: e0107524.
Minekus M, Smeets-Peeters M, Bernalier A, Marol-Bonnin S, Havenaar R, Marteau P, Alric M, Fonty G & Huis in't Veld JH (1999) A computer-controlled system to simulate conditions of the large intestine with peristaltic mixing, water absorption and absorption of fermentation products. *Appl Microbiol Biotechnol* **53**: 108-114.
Minh BQ, Schmidt HA, Chernomor O, Schrempf D, Woodhams MD, von Haeseler A & Lanfear R (2020) IQ-TREE 2: New Models and Efficient Methods for Phylogenetic Inference in the Genomic Era. *Mol Biol Evol* **37**: 1530-1534.
Monot M, Eckert C, Lemire A*, et al.* (2015) Clostridium difficile: New Insights into the Evolution of the Pathogenicity Locus. *Sci Rep* **5**: 15023.
Natarajan M, Walk ST, Young VB & Aronoff DM (2013) A clinical and epidemiological review of non-toxigenic Clostridium difficile. *Anaerobe* **22**: 1-5.
Olaitan AO, Dureja C, Youngblom MA*, et al.* (2023) Decoding a cryptic mechanism of metronidazole resistance among globally disseminated fluoroquinolone-resistant Clostridioides difficile. *Nat Commun* **14**: 4130.
Oliveira Junior CA, Silva ROS, Cruz DSG, Pires IH, Guedes RMC & Faria Lobato FC (2019) The non-toxigenic strain of Clostridioides difficile Z31 can prevent infection by C. difficile in experimental model piglets. *Anaerobe* **55**: 24-28.
Oliveira Junior CA, Silva ROS, Lage AP, Coura FM, Ramos CP, Alfieri AA, Guedes RMC & Lobato FCF (2019) Non-toxigenic strain of Clostridioides difficile Z31 reduces the occurrence of C. difficile infection (CDI) in one-day-old piglets on a commercial pig farm. *Vet Microbiol* **231**: 1-6.
Oliveira Paiva AM, Friggen AH, Hossein-Javaheri S & Smits WK (2016) The Signal Sequence of the Abundant Extracellular Metalloprotease PPEP-1 Can Be Used to Secrete Synthetic Reporter Proteins in Clostridium difficile. *ACS Synth Biol* **5**: 1376-1382.
Riedel T, Wetzel D, Hofmann JD*, et al.* (2017) High metabolic versatility of different toxigenic and non-toxigenic Clostridioides difficile isolates. *Int J Med Microbiol* **307**: 311-320.
Roseboom AM, Ducarmon QR, Hornung BVH, Harmanus C, Crobach MJT, Kuijper EJ, Vossen R, Kloet SL & Smits WK (2023) Carriage of three plasmids in a single human clinical isolate of Clostridioides difficile. *Plasmid* **125**: 102669.
Sambol SP, Skinner AM, Serna-Perez F, Owen B, Gerding DN & Johnson S (2023) Effective Colonization by Nontoxigenic Clostridioides difficile REA Strain M3 (NTCD-M3) Spores following Treatment with Either Fidaxomicin or Vancomycin. *Microbiol Spectr* **11**: e0051723.
Seemann T (2014) Prokka: rapid prokaryotic genome annotation. *Bioinformatics* **30**: 2068-2069.
Smits WK, Lyras D, Lacy DB, Wilcox MH & Kuijper EJ (2016) Clostridium difficile infection. *Nat Rev Dis Primers* **2**: 16020.
Soge OO, Beck NK, White TM, No DB & Roberts MC (2008) A novel transposon, Tn6009, composed of a Tn916 element linked with a Staphylococcus aureus mer operon. *J Antimicrob Chemother* **62**: 674-680.
Stojkovic V, Ulate MF, Hidalgo-Villeda F*, et al.* (2019) cfr(B), cfr(C), and a New cfr-Like Gene, cfr(E), in Clostridium difficile Strains Recovered across Latin America. *Antimicrob Agents Chemother* **64**.
Tansirichaiya S, Rahman MA & Roberts AP (2019) The Transposon Registry. *Mob DNA* **10**: 40.
Tonkin-Hill G, MacAlasdair N, Ruis C*, et al.* (2020) Producing polished prokaryotic pangenomes with the Panaroo pipeline. *Genome Biol* **21**: 180.
van den Belt M, Gilchrist C, Booth TJ, Chooi YH, Medema MH & Alanjary M (2023) CAGECAT: The CompArative GEne Cluster Analysis Toolbox for rapid search and visualisation of homologous gene clusters. *BMC Bioinformatics* **24**: 181.
van Eijk E, Anvar SY, Browne HP, Leung WY, Frank J, Schmitz AM, Roberts AP & Smits WK (2015) Complete genome sequence of the Clostridium difficile laboratory strain 630Deltaerm reveals differences from strain 630, including translocation of the mobile element CTn5. *BMC genomics* **16**: 31.
Villano SA, Seiberling M, Tatarowicz W, Monnot-Chase E & Gerding DN (2012) Evaluation of an oral suspension of VP20621, spores of nontoxigenic Clostridium difficile strain M3, in healthy subjects. *Antimicrob Agents Chemother* **56**: 5224-5229.
Viprey VF, Davis GL, Benson AD*, et al.* (2022) A point-prevalence study on community and inpatient Clostridioides difficile infections (CDI): results from Combatting Bacterial Resistance in Europe CDI (COMBACTE-CDI), July to November 2018. *Euro Surveill* **27**.
Wang S, Zhu D & Sun X (2022) Development of an Effective Nontoxigenic Clostridioides difficile-Based Oral Vaccine against C. difficile Infection. *Microbiol Spectr* **10**: e0026322.

670 Wang S, Heuler J, Wickramage I, Sun X & Uzal F (2022) Genomic and Phenotypic Characterization of the
671 Nontoxigenic Clostridioides difficile Strain CCUG37785 and Demonstration of Its Therapeutic Potential for the
672 Prevention of C. difficile Infection. *Microbiology Spectrum* **10**: e01788-01721.
673 Warny M, Pepin J, Fang A, Killgore G, Thompson A, Brazier J, Frost E & McDonald LC (2005) Toxin production by
674 an emerging strain of Clostridium difficile associated with outbreaks of severe disease in North America and
675 Europe. *Lancet (London, England)* **366**: 1079-1084.
676 Wiese M, Schuren FHJ, Smits WK*, et al.* (2022) 2'-Fucosyllactose inhibits proliferation of Clostridioides difficile
677 ATCC 43599 in the CDi-screen, an in vitro model simulating Clostridioides difficile infection. *Front Cell Infect*
678 *Microbiol* **12**: 991150.
679 Wishart DS, Han S, Saha S, Oler E, Peters H, Grant JR, Stothard P & Gautam V (2023) PHASTEST: faster than
680 PHASTER, better than PHAST. *Nucleic Acids Res* **51**: W443-W450.
681

682

683 **Table 1. Antimicrobial susceptibility of L-NTCD03**

684

Antibiotic	MIC (mg/L)[a]	EUCAST (T)ECOFF (mg/L)	Putatively associated AMR gene[b]
Augmentin	0.25	-	-
Cefuroxime	>256	-	*blaCDD*
Chloramphenicol	>256	-	*catP, cfr(*B*)*
Ciprofloxacin	>32	(32)	*gyrB*_S366A
Clindamycin	>256	16	*cfr*(B), *cplR*
Cotrimoxazole	0.06	-	-
Erythromycin	48	4	*erm*(52)
Fidaxomicin	0.06	0.5	-
Linezolid	6	-	*cfr*(B)
Meropenem	1	(8)	-
Metronidazole	0.06	2	-
Moxifloxacin	1	4	-
Penicillin	0.75	-	*blaCDD*
Rifampicin	>32	0.004	*rpoB*_R505K
Tetracycline	2	(0.25)	*tet*(M)
Teicoplanin	1	-	*vanZ1*
Vancomycin	0.38	2	-

685 [a] MICs were determined using Etest, except for fidaxomicin (where agar dilution was used) as described in

686 Materials and Methods

687 b EUCAST Epidemiological Cut-off (ECOFF) are given without, tentative epidemiological cut-off (TECOFF) values

688 are given within brackets (EUCAST, 2026).

689 [c] AMR gene content was determined using AMRFinderPlus (Feldgarden *et al.*, 2021). Genes not shown in table

690 are the aminoglycoside resistance genes *ant(6)-Ia*, *sat4*, *aph(3')-IIIa*, *blaAHM*, *nimB*-Cd. The latter is omitted

691 here for as the allele identified does not a contain the resistance associated promoter mutation (see

692 Discussion).

693

694

695

696

697

698

699 **Table 2. Table 1. Minimal inhibitory concentrations of *C. difficile* 630Δ*erm*-derived strains carrying different**

700 **plasmids.**

plasmid	antimicrobial MIC (mg/L)			
	clindamycin	linezolid	retapamulin	streptogramin A
pAP24 (control)	2	1	0.125	2
pIMM03 (*cfr*(B))	>256	12	16	16

701 Experiments were performed at n>3, with results consistent between experiments. Clindamycin and linezolid

702 MICs were determined by Etest, and MICs for retapamulin and streptogramin A were determined by modified

703 agar dilution (see Methods).

704

705

706 **Table 3**. **Oligonucleotides**

Oligonucleotide	Sequence (5'>3')	Reference
16S-F	TET[#]-GTGCGGCTGGATCACCTCCT	(Fawley *et al.*, 2015)
23S-R	CCCTGCACCCTTAATAACTTGACC	(Fawley *et al.*, 2015)
NF793	CACCTCCTTTTTGACTTTAAGCCTACGAATACC	(Fagan & Fairweather, 2011)
NF794	CACCGACGAGCAAGGCAAGACCG	(Fagan & Fairweather, 2011)
oIMM-001	CTACGGTACCCTCTACCTAATAGCCACAGGAG	This study
oIMM-002	GATGGGATCCTCACTGCATCCGCAATTC	This study
oIMM-003	GTTAATTGAGGAGTTTGGAGAATCG	This study
oIMM-004	CACATCTGATAATGGGTAGCGTTC	This study
oWKS-1070	GTCTTGGATGGTTGATGAGTAC	(Boekhoud *et al.*, 2020)
oWKS-1071	TTCCTAATTTAGCAGCAGCTTC	(Boekhoud *et al.*, 2020)
oWKS-1387	CAGATGAGGGCAAGCGGATG	(Boekhoud *et al.*, 2020)
oWKS-1388	CGTCGGTGAGCCAGAGTTTC	(Boekhoud *et al.*, 2020)

707 [#] TET: 5-tetrachlorofluorescein

708 **Figure Legends**

709

710 **Figure 1. L-NTCD03 is a non-toxigenic *C. difficile* strain. A.** L-NTCD03 does not show production of toxins in an
711 ELISA assay. The dotted line indicates the threshold value indicated by the manufacturer for defining toxin
712 production. **B**. Culture supernatant from L-NTCD03 does not lead to a reduction in transepithelial resistance as
713 measured in a Caco2/LS174T cellular model that was matured for 21 days (pre-exposure) before applying
714 culture supernatant (post exposure). **C**. Growth of L-NTCD03 is similar to other *C. difficile* strains. Colony
715 forming units (CFU) per milliliter culture were determined by a droplet-plating method. **D**. Spore formation of
716 L-NTCD03 is similar to other *C. difficile* strains. Spores were enumerated after ethanol treatment using a
717 droplet plating method. Values indicated are the mean and standard error of the mean of n=3 biological
718 replicates. LL-010 is a non-toxigenic control strain and LL-027 and LL-078 are toxigenic controls.

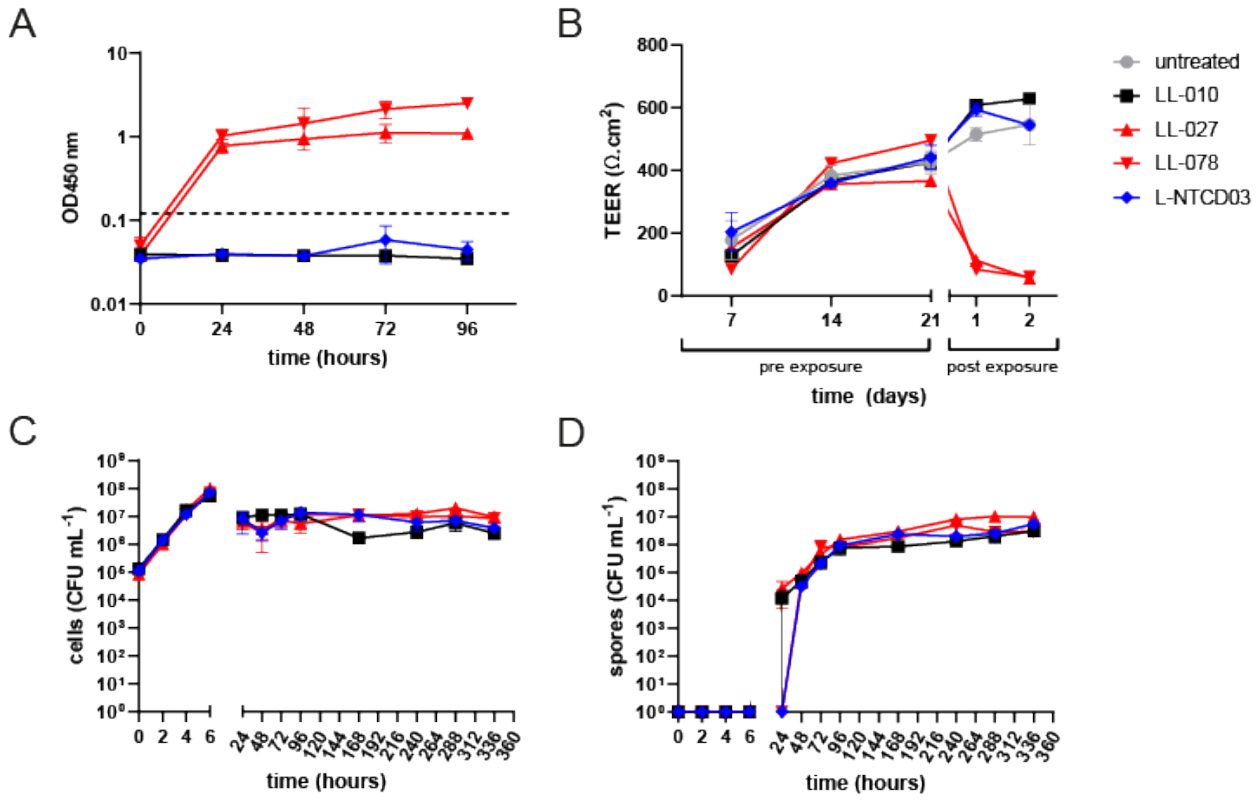

719

720

721 **Figure 2. L-NTCD03 does not induce pathology in the swine IsoLoop model. A.** Representative images from
722 histological analyses. Tissues samples were formalin fixed and paraffin embedded, sectioned and hematoxylin
723 and eosin stained. No significant *C. difficile*-associated lesions are observed in the control loop (an ileal loop
724 that was antibiotic-treated but not inoculated with *C. difficile*), normal ileum (not a loop but control for
725 surgical integrity of the loops) and the loop inoculated with L-NTCD03. In contrast, the loop inoculated with LL-
726 078 (toxigenic strain, positive control for *C. difficile* pathology) showed blunting of the villi with epithelial
727 necrosis, neutrophilic infiltration of lamina propria, and crypt abscesses. **B**. Combined histological scores for
728 the different samples. A bar plot depicting the mean histological score with standard error of the mean is
729 given, with individual datapoints depicted. Prespecified contrasts (see Supplementary Information) are shown
730 with brackets, with asterisks indicating the raw p-value magnitude, for readability (**: $p < 0.01$) , while
731 significance is determined by Holm adjustment across the three prespecified tests.
732

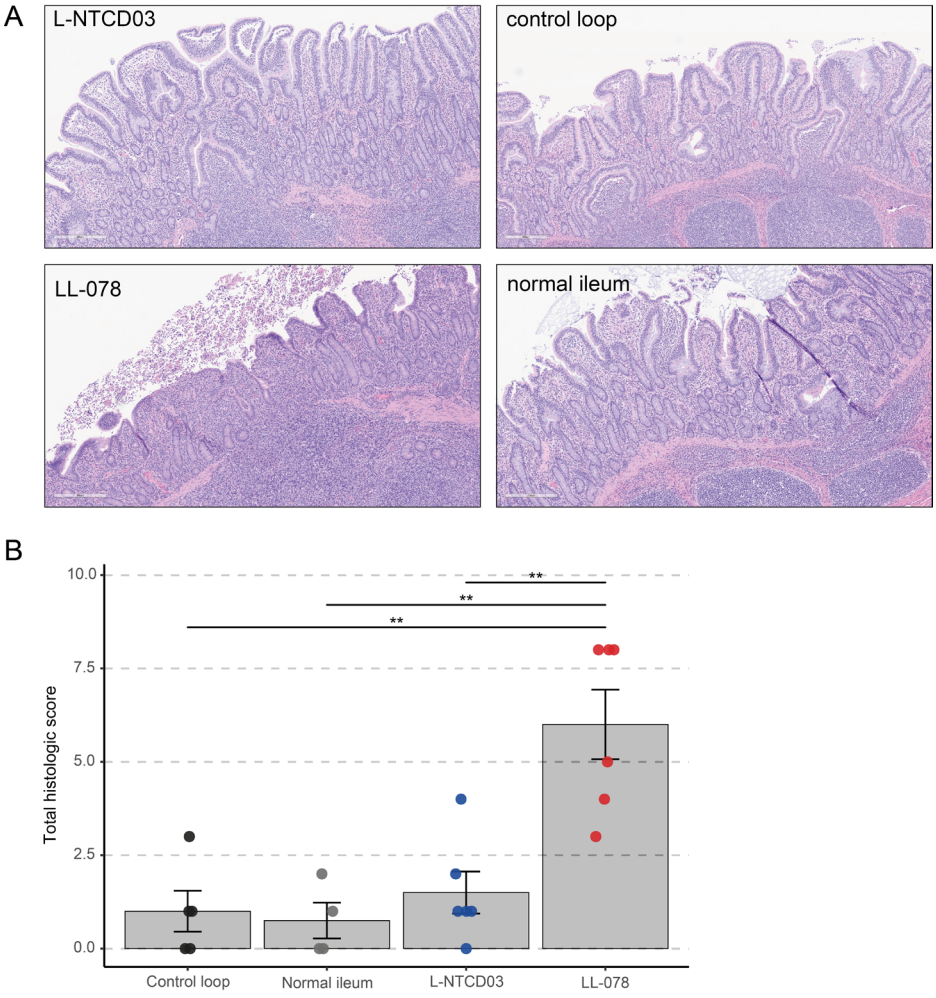

733
734

735 **Figure 3. L-NTCD03 harbors the novel transposon Tn*7696*.** Comparison of a region of the genome of L-NTCD03
736 with the genome of the closely related clade 4 strain DSM 29629 (GenBank NZ_CP016104). The insertion of
737 Tn*7696* into the *pdeR* gene (LLHAOGBK_00328 and LLHAOGBK_00311/CDIF29629_RS01565) is evident. Tn*7696*
738 harbors the tetracycline resistance gene *tet*(M) and an integrase (*int*-Tn), like Tn*916*. The gene with locus tag
739 LLHAOGBK_00319 (see main text) is abbreviated to 319 for simplicity. Colors and linkages indicate homology
740 between genes. *nox* encodes a predicted NADH dehydrogenase/nitroreductase (LLHAOGBK_00337/
741 CDIF29629_RS01610), *uvrA* an excinuclease (LLHAOGBK_00310/CDIF29629_RS01560) and *guaA* a glutamine-
742 hydrolyzing GMP synthase (LLHAOGBK_00305/CDIF29629_RS01525).
743

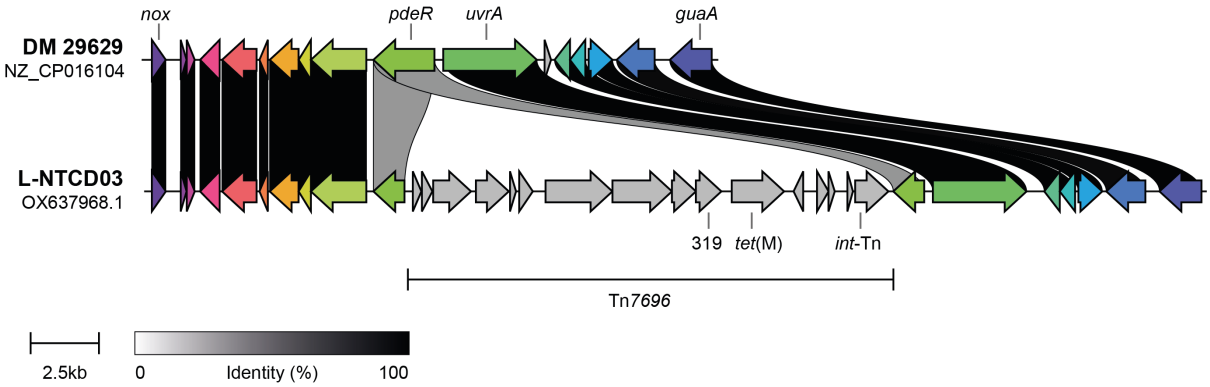

744
745

746 **Supplementary information**

747

748 **Histological scoring**

749 H&E-stained sections from each ileal loop were graded for four components present in the dataset: epithelial
750 necrosis, edema (mucosal/lamina propria), crypt abscess, and neutrophils in villi/lamina propria. A fifth field,
751 submucosal edema, was also recorded but was invariant (0 in this experiment) and therefore excluded from
752 totals.

753 Each component used an ordinal 0–5 scale with shared anchors; the best matching description was assigned:

754 • Epithelial necrosis: 0 = absent; 1–2 = scattered villus-tip necrosis; 3 = multifocal epithelial
755 lifting/patchy denudation; 4–5 = broad denudation/ulceration with diffuse surface loss.
756 • Edema (mucosal/lamina propria): 0 = none; 1–2 = subtle to mild expansion; 3 = clear expansion with
757 villus blunting; 4 = marked expansion; 5 = diffuse expansion with severe blunting/separation.
758 • Crypt abscess: 0 = none; 1–2 = rare crypts with a few intraluminal neutrophils/debris; 3 = several
759 crypts with clear pus; 4–5 = numerous/widespread abscesses across fields.
760 • Neutrophils in villi/lamina propria: 0 = no neutrophils; 1= scattered individual cells; 2 = multifocal
761 small clusters; 3 = multifocal large clusters; 4 = confluent clusters; 5 = sheets/near-diffuse infiltration.
762 (Field counts may aid consistency; final grade is by pattern/severity.)

763 Total histologic score: per loop, the sum of the four variable components (range 0–20); higher totals indicate
764 greater injury. Each loop was treated as the experimental unit; scoring was performed blinded to group
765 identity.

766

767 **Statistical analyses**

768 *Outcome and unit*. The primary endpoint was the total histologic score per ileal loop (range 0–20), computed
769 as the sum of four 0–5 ordinal components: epithelial necrosis, mucosal/lamina propria edema, crypt abscess,
770 and neutrophils in villi/lamina propria. Submucosal edema values were invariant and excluded from totals.
771 Each loop was the experimental unit; scoring was blinded to group.

772 *Descriptive statistics*. Group data are summarized as median [Q1–Q3]. Figures display mean ± SEM with per
773 loop jittered points.

774 *Global comparison*. Overall heterogeneity among Control loop, Normal Ileum, L-NTCD03 and LL-078 was
775 assessed with the Kruskal–Wallis test (two sided, $\alpha = 0.05$) using mid ranks with tie correction.
776 *Primary prespecified contrasts*. The biological comparisons of primary interest were LL-078 vs Control loop, LL-
777 078 vs Normal ileum, and LL-078 vs L-NTCD03. Each was tested using a two sided Mann–Whitney U test
778 (Wilcoxon rank sum). Multiplicity was controlled across these three tests using the Holm procedure (family
779 wise $\alpha = 0.05$). For each contrast we report the Holm adjusted p value and the rank biserial correlation (r) as an
780 effect size.
781

782 **Supplementary Table 1. Histopathological analysis of the pig-ileal loop experiments.**

	Epithelial necrosis	Edema	Crypt abscess	Submucosal edema	Neutrophils in villi/lamina propria	Total histological score
Control loop	0	0	0	0	0	0
Control loop	0	1	0	0	0	1
Control loop	0	1	1	0	1	3
Control loop	0	0	0	0	0	0
Control loop	0	1	0	0	0	1
Normal ileum	0	1	1	0	0	2
Normal ileum	0	0	0	0	0	0
Normal ileum	0	0	0	0	0	0
Normal ileum	0	1	0	0	0	1
L-NTCD03	1	1	1	0	1	4
L-NTCD03	0	1	0	0	0	1
L-NTCD03	0	0	0	0	0	0
L-NTCD03	0	1	1	0	0	2
L-NTCD03	0	1	0	0	0	1
L-NTCD03	0	1	0	0	0	1
LL-078	2	2	2	0	2	8
LL-078	2	2	2	0	2	8
LL-078	3	1	2	0	2	8
LL-078	2	1	1	0	1	5
LL-078	2	1	0	0	1	4
783 LL-078	1	1	0	0	1	3

784

785 **Supplementary Table 2. Antimicrobial resistance genes of L-NTCD03.**

Start	Stop	Strand	Locus tag	Resistance gene	Name	Class	Subclass	Alignment length	Reference length	Reference sequence	Coverage	Identity
4145	6043	+	LLHAOGBK_00005	gyrB_S366A	Clostridioides difficile quinolone resistant GyrB	quinolone	quinolone	633	633	WP_003434229.1	100	99,84
95557	99270	+	LLHAOGBK_00126	rpoB_R505K	Clostridioides difficile rifampin resistant RpoB	rifamycin	rifampin	1238	1238	WP_003436174.1	100	99,76
272459	274375	-	LLHAOGBK_00317	tet(M)	tetracycline resistance ribosomal protection protein Tet(M)	tetracycline	tetracycline	639	639	WP_000691736.1	100	99,69
334396	335442	+	LLHAOGBK_00374	cfr(B)	23SrRNA (adenine(2503)-C(8))-methyltransferase Cfr(B)	lincosamide/oxazolidinone/phenicol/pleuromutilin/streptogramin	chloramphenicol/clindamycin/linezolid/retapamulin/streptogramin B/virginiamycin	349	349	WP_002405682.1	100	99,71
526699	527319	+	LLHAOGBK_00554	catP	type A-11 chloramphenicol O-acetyltransferase CatP	phenicol	chloramphenicol	207	207	WP_002570989.1	100	100
548779	549684	+	LLHAOGBK_00577	ant(6)-Ia	aminoglycoside nucleotidyltransferase ANT(6)-Ia	aminoglycoside	streptomycin	302	302	WP_001255864.1	100	100
549684	550223	+	LLHAOGBK_00578	sat4	streptothricin N-acetyltransferase Sat4	streptothricin	streptothricin	180	180	WP_000627290.1	100	100
550319	551110	+	LLHAOGBK_00579	aph(3')-IIIa	aminoglycoside O-phosphotransferase APH(3')-IIIa	aminoglycoside	amikacin/kanamycin	264	264	WP_001096887.1	100	100
1530614	1532263	+	LLHAOGBK_01435	cplR	ABC-F type ribosomal protection protein CplR	lincosamide/pleuromutilin/streptogramin	clindamycin/lincomycin/retapamulin/virginiamycin	550	550	AJP12342.1	100	97,82
2811949	2812410	+	LLHAOGBK_02605	nimB-Cd	putative 5-nitroimidazole reductase NimB-Cd	nitroimidazole	nitroimidazole	154	155	CBE03766.1	99,35	100
3057328	3057834	-	LLHAOGBK_02836	vanZ1	glycopeptide resistance protein VanZ1	glycopeptide	vancomycin	169	169	CAJ68095.1	100	99,41
3344140	3345051	-	LLHAOGBK_03095	blaAHM	AHM family subclass B3-like metallo-beta-lactamase	beta-lactam	carbapenem	304	304	WP_011860980.1	100	97,7
3874110	3875045	-	LLHAOGBK_03550	blaCDD	CDD family class D beta-lactamase	beta-lactam	beta-lactam	312	308	WP_021361759.1	100	96,15
3965200	3966126	-	LLHAOGBK_03629	erm(52)	23SrRNA (adenine(2058)-N(6))-methyltransferase Erm(52)	macrolide	macrolide	309	309	WP_002571018.1	100	100

786